Impulse Radio NOMA Communications in 5G and Beyond

Mai T. P. Le, Giuseppe Caso, Luca De Nardis, Maria-Gabriella Di Benedetto

Department of Information Engineering, Electronics and Telecommunications, Sapienza University of Rome, Rome 00184, Italy.
Email: mai.le.it@ieee.org

Abstract

Motivated by recent theoretical challenges for 5G and beyond 5G systems, this chapter aims to position relevant results in the literature on code-domain non-orthogonal multiple access (NOMA) from an information-theoretic perspective, given that most of the recent intuition of NOMA relies on another domain, that is, the power domain. Theoretical derivations for several code-domain NOMA schemes are reported and interpreted, adopting a unified framework that focuses on the analysis of the NOMA spreading matrix, in terms of load, sparsity, and regularity features. The comparative analysis shows that it is beneficial to adopt extreme low-dense code-domain NOMA in the large system limit, where the number of resource elements and number of users grow unboundedly while their ratio, called load, is kept constant. Particularly, when optimum receivers are used, the adoption of a *regular* low-dense spreading matrix is beneficial to the system achievable rates, which are higher than those obtained with either *irregular* low-dense or dense formats, for any value of load. For linear receivers, which are more favorable in practice due to lower complexity, the *regular* low-dense NOMA still has better performance in the underloaded regime (load < 1), while the *irregular* counterpart outperforms all the other schemes in the overloaded scenario (load > 1).

1 Introduction

Being acknowledged as an important enabler for 5G multiple access, non-orthogonal multiple access (NOMA) with its diverse dialects recently attracted a huge attention in the wireless community from both industry and academia [1]. In fact, NOMA has been currently proposed by the 3rd Generation Partnership Project (3GPP) for 5G New Radio (NR). Many NOMA schemes for NR were initially proposed in Release-13 (Rel-13) Study Item, and were partly analyzed in Rel-14. While some specifications of 5G-NR have been officially standardized in the current Rel-15 (for example, Specification TS 38.211 for Physical channels and modulation [2]), Specification TS 38.812 for Study on NOMA for

NR [2] is still under investigation with the expectation to have a 'ready' NR system in 2020 [3]. Furthermore, NOMA is a strong candidate for beyond 5G systems, thanks to its capability of supporting massive communications [4]. In traditional orthogonal multiple access (OMA) schemes, users are allocated to orthogonal resource elements (REs) either in time, frequency, or code domains [5]. Based on the relationship between the number of users K and the number of REs N, also called degrees of freedom, the system is termed *underloaded* when $K < N$ and *overloaded* when $K > N$. As a matter of fact, one should note that underloaded systems can be made OMA under the assumptions of perfect knowledge of channel state information and perfect synchronization between the transmitters and receivers. A very different situation arises when the system is overloaded. Even under ideal conditions such as ideal propagation and ideal allocation strategy, the system is intrinsically affected by 'collisions' due to interference [6]. This scenario may be easily envisioned in 5G, for example in the internet-of-things (IoT), in which a huge number of terminals are required to transmit simultaneously. Noteworthy that, according to this understanding, all conventional OMA schemes, including the well-known CDMA, become NOMA in the overloaded regime, due to the exceedingly large number of users compared to the number of REs.

In order to enable detection at the receiver side, different users are detected based on the difference of power or spreading codes, leading to two main corresponding approaches: power-domain NOMA vs. code-domain NOMA. To address interference provoked by the lack of a sufficient number of REs, controllable interference among REs may be introduced in the code domain with an acceptable complexity of receivers [8]. This NOMA approach is currently known as *code-domain NOMA* [5]. However, with reference to NOMA, most of recent works in the literature focus on the power-domain case [1], which is based on the idea of serving multiple users at the same time/frequency/code with different power levels [1, 5, 9]. This chapter, on the other hand, makes an effort to contribute to the understanding of code-domain approach, particularly from an information-theoretic perspective.

In the context of massive connectivity, expected for 5G and beyond 5G systems, the number of users is supposed to be very large compared to the number of REs. The behavior of the system should thus be considered in the asymptotic limit, where both K and N go to infinity, while the ratio $K/N = \beta$, called load, remains finite. This corresponds to analyzing the system in the *large system limit* (LSL) [10]. NOMA schemes and corresponding achievable rates can be investigated in the LSL considering three main features:

- load β, particularly $\beta > 1$, also known as overloading factor, which is considered as a significant feature of code-domain NOMA [5].
- sparsity, describing the structure of code-domain NOMA spreading matrix, whose spreading sequence is commonly designed to be sparse to reduce the detection complexity [5].
- regularity, which characterizes possible spreading mapping constraints [11]. As will be detailed in Sec. 3, *regular* low-dense NOMA refers to

the case where the number of users per occupied RE and the number of occupied REs per user are fixed, whereas *irregular* designates the case where these numbers are random and fixed on average [11, 12, 13].

This chapter addresses a general code-domain NOMA analysis by mapping relevant information-theoretic results in the literature on code-domain NOMA, from which the corresponding information-theoretic results are expected to explore the relationship between the achievable rates and the aforementioned peculiar features of code-domain NOMA. Understanding the behavior of the system in terms of information-theoretic bounds can provide crucial insight to select system parameters, and can contribute as a reference for future release of 5G standardization [5].

2 A reference mathematical model for Code-domain NOMA

Apart from the fact non-orthogonality feature of NOMA has been used recently [1], initial NOMA concept has a long story from the beginning of 1990s. Non orthogonal signal sets with particular structures were invented such that they may be detectable at the receiver. First investigations on designing guidelines for non-orthogonal spreading codes were made by Ross and Taylor [14, 15] that were applicable to an overloading system. By adding additional linearly dependent codes while maintaining the orthogonal minimum distance (Euclidean distance) to ensure feasible detection, the signal sets essentially became non-orthogonal. In addition, these sets were put under the constraint as such all users should not have higher powers than that of orthogonal set. On the receiver side, iterative decoding algorithm such as message passing algorithm (MPA) detector, also known as belief propagation (BP) algorithm in low-density parity-check (LDPC) codes, is employed.

CDM-NOMA exploits code to distinguish different users at the receiver, i.e. it function similarly to the traditional DS-CDMA system. The main feature identifying CDM-NOMA from CDMA is by employing sparsity in spreading sequences via low-density or low cross-correlation sequences. Based on the specific scenario, single-carrier or multi-carrier NOMA schemes can be adopted, corresponding to single-carrier DS-CDMA or multi-carrier CDMA (MC-CDMA), respectively. The 15 existing proposals of NOMA proposed for the Rel-14 3GPP NR Study item [2] (Table 1) and recent CDM-NOMA proposals available in the literature, therefore, will be classified based on dense vs. low-dense and single vs. multi carrier features.

In addition to proposed methods for NOMA from Table 1, including MUSA [16], PDMA [17, 18], IGMA [19], IDMA [20, 21], other NOMA schemes such as LDS-CDMA [22] (also known as time-hopping (TH-CDMA) [23, 24]), SAMA [25] will be shown tightly correlated to traditional single-carrier DS-CDMA, therefore, are classified as single-carrier NOMA. By contrast, LDS-OFDM [26, 27], along with remained NOMA schemes in Table 1 including SCMA [28, 29],

	NOMA schemes	Full Name	Company	UL/DL
1	Power-domain NOMA	Power-domain non-orthogonal multiple access	DCM	UL/DL
2	SCMA	Sparse code multiple access	Huawei	UL/DL
3	MUSA	Multi-user shared access	ZTE	UL/DL
4	PDMA	Pattern division multiple access	CATT	UL/DL
5	LSSA	Low code rate and signature based shared access	ETRI	UL
6	RSMA	Resource spread multiple access	Qualcomm	UL
7	IGMA	Interleave-grid multiple access	Samsung	UL/DL
8	IDMA	Interleave division multiple access	Nokia	UL
9	NCMA	Non-orthogonal coded multiple access	LGE	UL
10	NOCA	Non-orthogonal coded access	Nokia	UL
11	GOCA	Group orthogonal coded access	MTK	UL
12	LDS-SVE	Low density spreading - signature vector extension	Fujitsu	UL/DL
13	FDS	Frequency domain spreading	Intel	UL
14	LCRS	Low code rate spreading	Intel	UL
15	RDMA	Repetition division multiple access	MTK	UL

TABLE 1: NOMA schemes proposed for the Rel-14 3GPP NR Study Item [2]

LSSA [30], NCMA [31], NOCA [32], GOCA [33], LDS-SVE [34], LCRS/FDS [35], RDMA [33] are well fitted to multi-carrier CDMA model, hence, classified here as multi-carrier NOMA. RSMA [36, 37] is a NOMA dialect that is proposed for both type of waveforms, depending on the specific application scenario.

Code-domain NOMA classification is illustrated in Fig. 1.

2.1 Single-carrier NOMA

For single-carrier NOMA, each data symbol of user k is spread by N chips of the corresponding spreading sequence, that is similar to as DS-CDMA system. Naturally, the mathematical model of single-carrier NOMA may be built from the baseline model of DS-CDMA, proposed by Verdú and Shamai in [10] and [38] as follows

$$\boldsymbol{y} = \boldsymbol{S}\boldsymbol{H}\boldsymbol{b} + \boldsymbol{n}, \tag{1}$$

where the received signal $\boldsymbol{y} \in \mathbb{C}^N$ belongs to a space characterized by N signal dimensions. Note that N also represents the number of elements over which

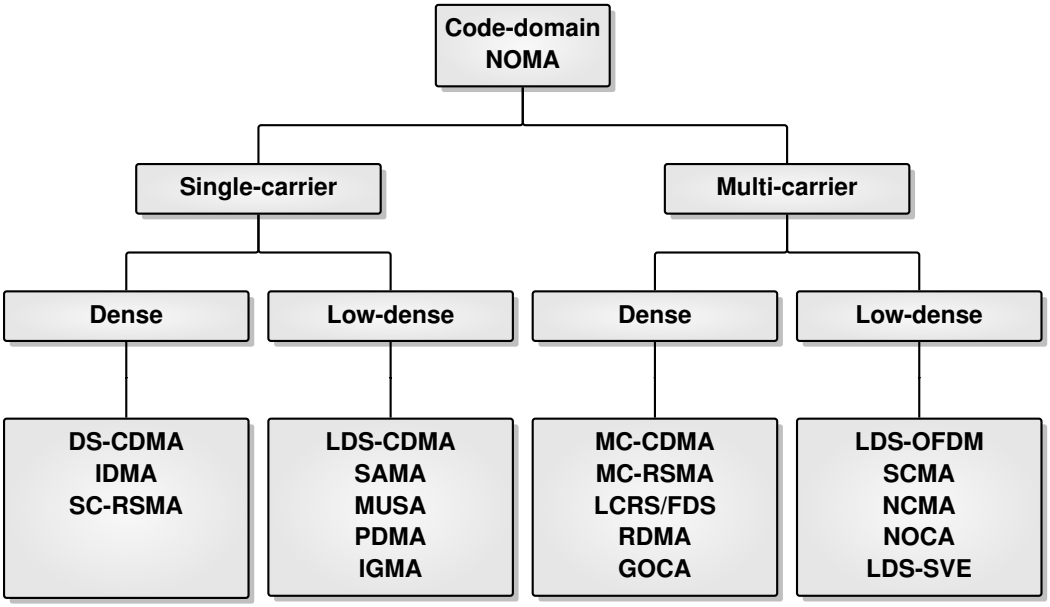

FIGURE 1: Code-domain NOMA classfification

each symbol is spread, that is the number of REs, and equivalent to the number of 'chips', as termed commonly in CDMA. Vector $\boldsymbol{b} = [b_1, \ldots, b_K]^T \in \mathbb{C}^K$ is the vector of symbols transmitted by K users. Being a random spreading matrix, $\boldsymbol{S} = [\boldsymbol{s}_1, \ldots, \boldsymbol{s}_K] \in \mathbb{C}^{N \times K}$ is composed of K columns, each being the spreading sequence $\mathbf{s}_k$ of user k $(1 \leqslant k \leqslant K)$. Supposing the channel is flat, the channel matrix can be represented as $\boldsymbol{H} = \text{diag}\,[h_1, \ldots, h_K] \in \mathbb{C}^{K \times K}$, whereas it reduces to the identity matrix if the AWGN channel is assumed. Lastly, the noise $\boldsymbol{n} \in \mathbb{C}^N$ is described by a circularly-symmetric Gaussian vector with zero mean and covariance $N_0\boldsymbol{I}$.

The nature of the representation matrix $\boldsymbol{S}$ defines the multiple access methods. This matrix is known as spreading matrix or signature matrix in DS-CDMA, TH-CDMA, LDS-CDMA, SAMA, or code matrix in MUSA, and pattern matrix in PDMA. As a matter of fact, NOMA schemes can be classified into dense vs. low-dense, where the corresponding matrix $\boldsymbol{S}$ is dense if all REs are used vs. low-dense, when some REs are not used. In terms of energy, this corresponds to having all REs contain signal energy vs. energy is concentrated on only part of the available REs, reflected by the presence of nonzero entries in $\boldsymbol{S}$. According to this understanding, DS-CDMA inherently stands for dense spreading. For single-carrier NOMA, the dense group includes DS-CDMA and IDMA, while the low-dense group includes LDS-CDMA, TH-CDMA, SAMA, MUSA, IGMA and PDMA.

2.2 Multi-carrier NOMA

For multi-carrier NOMA schemes, the system can be described as a combination of CDMA for dense NOMA (respective, LDS-CDMA for low-dense NOMA) with multi-carrier modulation, for e.g. OFDM, that makes multi-carrier NOMA work analogously to MC-CDMA [39]. Based on this intuition, the system model of multi-carrier NOMA basically can be elaborated as below, assuming the number of OFDM subcarriers shared by every user is also equal to the spreading gain N [40].
In multi-carrier NOMA, each data symbol of user k is replicated into N parallel copies, each copy is then multiplied by a chip from the respective spreading sequence. All N copies are then mapped to N subcarriers and are transmitted in parallel. Thanks to inverse discrete Fourrier transform (IDFT) implementation, those N parallel chips are converted into serial sequence for further transmission [40].

Adopting the same notation of spreading matrix $\boldsymbol{S} = [\boldsymbol{s}_1, \ldots, \boldsymbol{s}_K]$ with $\boldsymbol{s}_k$ being frequency-domain spreading sequence of user k as in eq. (1), the baseband signal by the kth user in time-domain is expressed by

$$\boldsymbol{W}\boldsymbol{s}_k b_k.$$

Here $\boldsymbol{W}$ denotes the $N \times N$ IDFT matrix, and b_k again stands for the data symbol of the kth user.

As a matter of fact, the receiver consists of N matched filters, corresponding to N subcarriers, is equivalently to conducting a discrete Fourrier transform (DFT) on the discrete baseband domain. Therefore, the received vector by user k in the frequency domain is $b_k \tilde{\boldsymbol{s}}_k$, where

$$\tilde{\boldsymbol{s}}_k = \mathrm{diag}[h_1^1, \ldots, h_k^N]\boldsymbol{s}_k,$$

with h_k^i being the fading coefficient at subcarrier i of the kth user.

Since in practice, each subcarrier is narrow enough to experience only flat fading, the system model of multi-carrier NOMA is, therefore, mathematically equivalent to that of single-carrier NOMA in (1) with respect to flat-frequency fading. This observation is also reported by Tulino *et al.* [40] for the case of DS-CDMA and MC-CDMA. Here the spreading matrix $\boldsymbol{S} \in \mathbb{C}^{N \times K}$ again defines different multi-carrier NOMA schemes.

3 Theoretical analysis of Code-domain NOMA

In this section, the theoretical behavior of NOMA is analyzed under the impact of three main factors, that are: load, sparsity and regularity. First, the load factor provides a straightforward way to study the system behavior in the underloaded ($\beta < 1$) vs. overloaded ($\beta > 1$) regimes. As mentioned above, overloaded systems are necessarily NOMA, since as soon as β overcomes the boundary value $\beta = 1$, new users find all REs occupied.

The second feature, sparsity, evaluates system from dense to extreme low-dense based on N_s, the number of used dimensions, defines as the *degree of sparseness*. If $N_s = N$, the system is dense. If $N_s = 1$, then the system is extreme low-dense. All other degrees of sparseness lie in between these two extreme cases. The dense vs. low-dense feature is directly reflected by the properties of matrix $\boldsymbol{S}$, where '0' in the matrix indicates elements with zero energy. A heuristic way to think of NOMA scheme is thus as a version of the overloaded CDMA scheme and low-dense NOMA can be referred to as sparse overloaded CDMA [41]. Naturally, it is expected to investigate the effect of those NOMA parameters, including the load β and the degree of sparseness N_s, on theoretical behavior of dense vs. low-dense NOMA.

Achievable rates of low-dense NOMA in the LSL were early and extensively evaluated via sparse CDMA by means of the replica method, also known as heuristic statistical physics, in [41, 42, 11, 43]. Since the derivations provided by replica method were typically non-rigorous, the information-theoretic analyses on low-dense NOMA were found rigorously via closed-form expressions in LDS/TH-CDMA model [23, 24], and in regular sparse NOMA model [12, 13]. Given that multiple system models are possibly proposed due to different assumptions, below we reported all curves along with the existing relevant theoretical results in our unified model (c.f. 2).

Regarding the third feature, the regularity, low-dense NOMA ($N_s < N$) are further classified into *irregular* vs. *regular* based on spreading mapping constraints, given that N_s is also the number of *occupied* REs per user, whereas N is the total number of REs per user. Previous works on sparse CDMA and low-dense NOMA were classified as *irregular* since the number of occupied REs per user was randomly Poissonian distributed with fixed mean [41, 42], and randomly uniformly distributed [23, 24][1], respectively. On the other hand, in terms of spreading matrix, the regularity assumption in [12, 13] requires matrix $\boldsymbol{S}$ be structured with exactly $N_s \in \mathbb{N}^+$ and $\beta N_s \in \mathbb{N}^+$ non-zero entries per column and row, respectively. It is equivalent to have each user occupying N_s REs and each RE being allocated with exact βN_s users, subject to N_s and βN_s being integers. It is, in general, challenging to have such an ideal model in practical scenarios where users are not allowed to independently select the spreading sequences, they must be coordinated or central scheduled [12]. The *regular* low-dense NOMA via *regular* sparse CDMA was early demonstrated to be superior to the dense in terms of bit error rate in high noise regime in [11], and in terms of spectral efficiency via explicit analytical expressions in recent works [12, 13].

In the following, theoretical behavior of *irregular* vs. *regular* low-dense NOMA ($N_s < N$) is analyzed with the adopted reference models LDS/TH-CDMA [23, 24] vs. regular sparse NOMA [12, 13], respectively. DS-CDMA is adopted as a representative of the dense NOMA group ($N_s = N$) [38]. Both optimal and linear receivers are considered in all cases. Spectral efficiency expressions [bits/s/Hz] for different cases are reported for the self-contained purpose

[1]The irregular low-dense NOMA in [23, 24] is called as *partly-regular* sparse NOMA in [12, 13].

TABLE 2: Summary of available theoretical bounds with corresponding references in the literature

	Dense NOMA ($N_s = N$)	Low-dense NOMA ($1 < N_s < N$)		Low-dense NOMA ($N_s = 1$)	
		Irregular	Regular	Irregular	Regular
Literature	[38]	[23]	[13]	[23]	[7]

of the chapter. It is important to notice that the theoretical results of *irregular* low-dense NOMA are available only for $N_s = 1$ [23, 24], while closed-form expressions of the *regular* case are valid only for intermediate degrees of sparseness, specifically for $N_s \geqslant 2, \beta N_s \in \mathbb{N}^+$ [13]. For *irregular* low-dense NOMA, since the closed-form expressions for intermediate N_s do not exist yet in the literature (and in general, are not easy to achieve), the results will be shown via Monte Carlo simulations for a full coherent overview. For *regular* low-dense NOMA, the regularity in case of $N_s = 1$ yields a typical setting, which includes a set of parallel Gaussian multiple access channels (MAC), that has been recently investigated in [7]. The references for mapping information-theoretic results in code-domain NOMA are summarized in Table 2, with the corresponding literature.

3.1 Dense vs. *Irregular* low-dense NOMA

In this part, theoretical behavior of dense vs. *irregular* low-dense NOMA is analyzed with the two corresponding reference models, that are DS-CDMA ($N_s = N$) [38] and LDS/TH-CDMA ($N_s < N$) [23]. Since the AWGN channel is used for both cases, the channel matrix $\boldsymbol{H}$ in eq. (1) becomes an identity matrix. The *only difference* in the mathematical model between DS-CDMA and LDS-CDMA is situated in the sparseness of matrix $\boldsymbol{S}$. In DS-CDMA ($N_s = N$), all entries of $\boldsymbol{S}$ are randomly filled by binary values of $\{\pm 1\}$, while in LDS-CDMA, for example with $N_s = 1$, each column of $\boldsymbol{S}$, representing a user, contains only *one* nonzero entry ($\{+1\}$ or $\{-1\}$), and all the rest are nil.

Figure 2 shows the achievable rates of dense vs. *irregular* low-dense systems with optimum and linear receivers as a function of β with fixed value of $E_b/N_0 = 10$ [dB]. With respect to load factor β, the border line (vertical dashed line) at $\beta = 1$ divides Fig. 2 into two areas corresponding to OMA (underloaded with $\beta < 1$) and NOMA (overloaded with $\beta > 1$), with dark and light shaded area, respectively.

In the LSL, Fig. 2 shows that for optimum receivers, dense systems always outperform *irregular* low-dense, irrespective of β, that is, whether OMA or NOMA. Achievable rates for the *irregular* type drop with N_s from the dense case ($N_s = N$) to the extreme low-dense case ($N_s = 1$), and the gap between the *irregular* low-dense and dense becomes negligible at $N_s = 2$, and tends to vanish from $N_s > 2$, e.g. $N_s = 5$. On the other hand, the behavior of linear detection

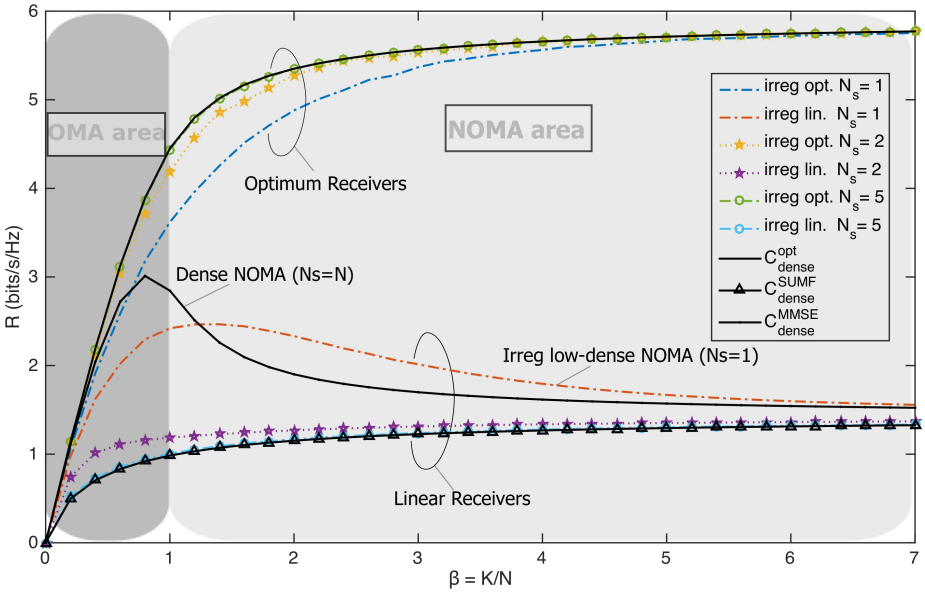

FIGURE 2: Achievable rates (bits/s/Hz) of dense NOMA vs. *irregular* low-dense NOMA as a function of β with fixed $E_b/N_0 = 10$ [dB] (parts of the data used to draw this figure were extracted from [23])

changes, with respect to the level of density of the system. For MMSE receivers, achievable rates of the dense systems are higher than the *irregular* low-dense in the OMA area, while this situation is inverse in the NOMA area, starting from about $\beta > 1.2$. With growing N_s, for example $N_s = \{2, 5\}$, the gap between the achievable rates of *irregular* low-dense NOMA with the SUMF receiver and dense NOMA, sharply reduces, to converge to the SUMF dense curve. Given that optimum detection is unfeasible to implement in practice due to the receiver complexity, the above observation provides the ground for suggesting *irregular* low-dense NOMA in the LSL, for example, for *irregular* low-dense case with $N_s = 1$.

The reported analysis holds in the case of flat-fading channel, as investigated and proved in [24].

3.2 Dense vs. *Regular* low-dense NOMA

Theoretical analysis of *regular* low-dense NOMA is investigated in this part, in comparison with the dense case.

- $1 < N_s < N$: Closed-form expressions of *regular* low-dense NOMA achievable rates for both optimum and MMSE receivers in [13] are valid under the following constraints:
  - if each user has $2 \leq N_s \in \mathbb{N}^+$ non-zero entries in its spreading

sequence, $2 \leq \beta N_s \in \mathbb{N}^+$ users shoud be assigned in the same RE;
  - spreading matrix $\boldsymbol{S}$ is assumed to converge to a bipartite Galton-Watson tree in the LSL (see ([13], Theorem 2) for a full description).

  To effectively induce non integer values of N_s and βN_s, one may employ time-sharing between different $(N_s, \beta N_s)$ points in the admissible set to achieve the same total throughput as mentioned in ([13], Remark 4).

- $N_s = 1$: The regularity imposes $\beta \in \mathbb{N}^+$ users per each RE, that is equivalent to having a set of N parallel Gaussian MAC channels [7]. This observation may bring more insight on the behavior of the *regular* with respect to optimum and linear receivers.

Figure 3 shows the achievable rates of MMSE, ZF, SUMF receivers for the dense ($N_s = N$), LMMSE receiver for the *regular* low-dense schemes with $N_s = \{1, 2, 5\}$. The linear receiver for the *irregular* low-dense NOMA with the typical case $N_s = 1$ is also shown for comparison. In contrast to the *irregular* counterpart, achievable rates for the *regular* low-dense NOMA, which are superior to all other cases, grow gradually for lower values of $N_s < N$, and reach the ultimate rate (Cover-Wyner bound) when $N_s = 1$.
The reason that makes the optimal spectral efficiency of the *irregular* low-dense to be lower than the dense case may be caused by the random nature of user-resource allocation, leading to a condition in which some users are not assigned with any RE, while some REs are left unused. On the other hand, the regularity feature of the *regular* low-dense NOMA contributes to increasing the optimal spectral efficiency by employing user-mapping intentionally. Nonetheless, this also imposes as a direct consequence additional practical challenges in having some kind of coordination while allocating the resources to users [12, 13].
For linear receivers, a remarkable observation from low-dense NOMA with $N_s = 1$ can be given: capacity of *regular* low-dense NOMA outperforms all the rest when $\beta \leqslant 1$ (OMA area), particularly to the typical setting when $N_s = 1$; while in the overloaded regime (NOMA area), there is an intersection where capacity of *irregular* low-dense NOMA with $N_s = 1$ outperforms all other cases. By numerical equation solving, the exact value of the intersection is located at $\beta = 1.232$, from which *irregular* low-dense NOMA with $N_s = 1$ dominates those of dense NOMA, as well as with all other degrees of sparseness ($N_s > 1$) till about $\beta \approx 5$, and then tend to converge for $\beta > 5$ (with the negligible gap of about 5% at $\beta = 5$). These observed results can be used as a driving rationale in system design.

4 Conclusion

Motivated by the key challenge of finding and analyzing theoretical bounds for NOMA in massive communications, this chapter sheds some light on the relationship between achievable rates and NOMA parameters, such as load factor, degree of sparseness and regularity. A unified framework for several code-domain

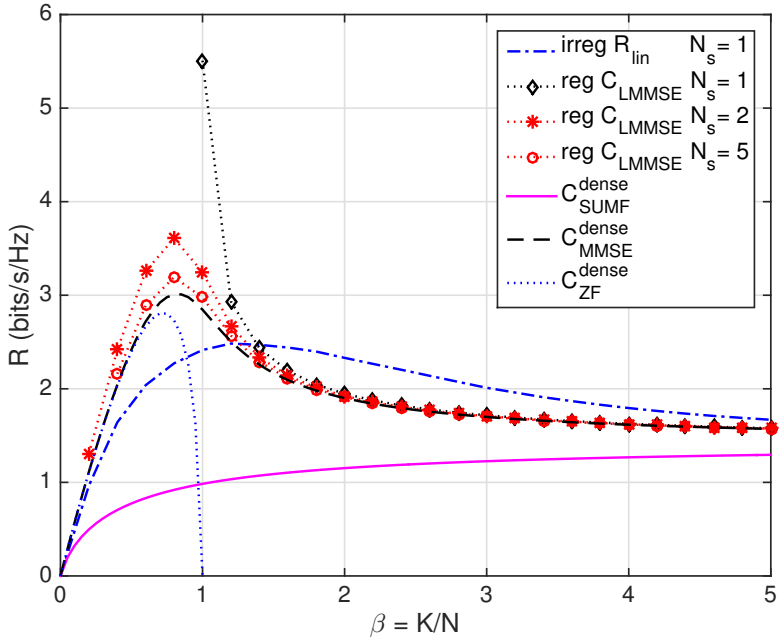

FIGURE 3: Achievable rates (bits/s/Hz) of dense NOMA ($N_s = N$) with SUMF, MMSE, ZF receivers vs. low-dense NOMA ($N_s = 1, 2, 5$) with linear receivers as a function of β for fixed $E_b/N_0 = 10$ [dB]

NOMA schemes was presented. The analytical framework, built on the traditional DS-CDMA model, proved to be flexible enough for representing several code-domain dialects, and, in particular, addressed properties of a fundamental element of the model, that is, the representation matrix $\boldsymbol{S}$.

Theoretical investigations were interpreted in the LSL for both optimum and linear receivers, based on closed-form expressions existing for three distinctive cases, that are, dense vs. *regular* low-dense and *irregular* low-dense NOMA, corresponding to DS-CDMA ($N_s = N$) [38] vs. LDS-CDMA ($N_s = 1$) [23] and *regular* sparse NOMA ($2 \leq N_s \in \mathbb{N}^+, \beta N_s \in \mathbb{N}^+$) [13]. For any value of load, low-dense NOMA cases were shown to be more spectral-efficient than dense ones. For optimum receivers, achievable rates of the *regular* low-dense are higher than the *irregular* low-dense and dense NOMA regardless of load. To this end, the system must be constrained to have exactly N_s REs per user and $\beta N_s \in \mathbb{N}$ users per resource; this imposes either central scheduling or users coordination. For linear receivers, spectral efficiency of *regular* low-dense NOMA was proved to be higher than all the other cases in the underloaded regime, while spectral efficiency of *irregular* low-dense dominated other NOMA cases in the overloaded systems, particularly when the system load β is within an interval that is about [1.2, 5]. When N_s increases, that is sparseness decreases, achievable rates of

low-dense cases rapidly converged to achievable rates of the dense case, as soon as $N_s = 2$.

In conclusion, by changing the spreading strategy from dense to low-dense, specific theoretical limits hold, showing that, to obtain higher achievable rates for linear decoders while still enjoying the lower receiver complexity, it is advisable to adopt sparse communications, and in particular *irregular* extreme low-dense schemes when systems are overloaded and *regular* extreme low-dense cases in the underloaded regime.

References

[1] Z. Ding, X. Lei, G. K. Karagiannidis, R. Schober, J. Yuan, and V. K. Bhargava, "A survey on non-orthogonal multiple access for 5g networks: Research challenges and future trends," *IEEE J. Sel. Areas Commun.*, vol. 35, no. 10, pp. 2181–2195, Oct. 2017.

[2] 3rd Generation Partnership Project (3GPP) Portal, 2017, [Online]. Available: https://portal.3gpp.org/, accessed on May 09, 2018.

[3] S.-Y. Lien, S.-L. Shieh, Y. Huang, B. Su, Y.-L. Hsu, and H.-Y. Wei, "5G New radio: Waveform, Frame Structure, Multiple Access, and Initial Access," *IEEE Trans. Commun.*, vol. 55, no. 6, pp. 64–71, June 2017.

[4] Y. Liu, Z. Qin, M. Elkashlan, Z. Ding, A. Nallanathan, and L. Hanzo, "Nonorthogonal multiple access for 5g and beyond," *Proceedings of the IEEE*, vol. 105, no. 12, pp. 2347–2381, Dec 2017.

[5] L. Dai, B. Wang, Y. Yuan, S. Han, C. l. I, and Z. Wang, "Non-orthogonal multiple access for 5G: solutions, challenges, opportunities, and future research trends," *IEEE J. Sel. Areas Commun.*, vol. 53, no. 9, pp. 74–81, Sept. 2015.

[6] R. E. Learned, A. S. Willsky, and D. M. Boroson, "Low complexity optimal joint detection for oversaturated multiple access communications," *IEEE Trans. Signal Process.*, vol. 45, no. 1, pp. 113–123, Jan. 1997.

[7] M. T. P. Le, G. C. Ferrante, G. Caso, L. De Nardis, and M.-G. Di Benedetto, "On information-theoretic limits of code-domain NOMA for 5G," *IET Communications*, vol. 12, no. 15, pp. 1864–1871, 2018.

[8] J. G. Andrews, "Interference cancellation for cellular systems: a contemporary overview," *IEEE Wireless Commun. Mag.*, vol. 12, no. 2, pp. 19–29, 2005.

[9] Z. Ding, Y. Liu, J. Choi, Q. Sun, M. Elkashlan, I. Chih-Lin, and H. V. Poor, "Application of non-orthogonal multiple access in LTE and 5G networks," *IEEE Commun. Mag.*, vol. 55, no. 2, pp. 185–191, Feb. 2017.

[10] S. Shamai and S. Verdú, "The impact of frequency-flat fading on the spectral efficiency of CDMA," *IEEE Trans. Inf. Theory*, vol. 47, no. 4, pp. 1302–1327, May 2001.

[11] J. Raymond and D. Saad, "Sparsely spread CDMA- a statistical mechanics-based analysis," *J. Phys. A: Math. Theor.*, vol. 40, no. 41, pp. 12 315–12 333, 2007.

[12] O. Shental, B. M. Zaidel, and S. S. Shitz, "Low-density code-domain NOMA: Better be regular," in *Proc. IEEE Int. Symp. Inf. Theory (ISIT)*, 2017, pp. 2628–2632.

[13] B. M. Zaidel, O. Shental, and S. Shamai, "Sparse NOMA: A Closed-Form Characterization," in *Proc. IEEE Int. Symp. on Inf. Theory (ISIT)*, Vail, CO, USA, June 2018, pp. 1106–1110.

[14] J. A. F. Ross and D. P. Taylor, "Vector assignment scheme for $m+n$ users in n-dimensional global additive channel," *Electronics Letters*, vol. 28, no. 17, pp. 1634–1636, 1992.

[15] ——, "Multiuser signaling in the symbol-synchronous AWGN channel," *IEEE Trans. Inf. Theory*, vol. 41, no. 4, pp. 1174–1178, 1995.

[16] Z. Yuan, G. Yu, W. Li, Y. Yuan, X. Wang, and J. Xu, "Multi-user shared access for internet of things," in *Proc. IEEE Veh. Technol. Conf. (VTC-Spring)*, Nanjing, 2016, pp. 1–5.

[17] S. Chen, B. Ren, Q. Gao, S. Kang, S. Sun, and K. Niu, "Pattern Division Multiple Access- A Novel Nonorthogonal Multiple Access for Fifth-Generation Radio Networks," *IEEE Trans. Veh. Technol.*, vol. 66, no. 4, pp. 3185–3196, Apr. 2017.

[18] J. Zeng, B. Li, X. Su, L. Rong, and R. Xing, "Pattern division multiple access (PDMA) for cellular future radio access," in *Proc. IEEE Int. Conf. on Wireless Commun. and Signal Process. (WCSP)*, Nanjing, China, 2015, pp. 1–5.

[19] 3rd Generation Partnership Project (3GPP), *Non-orthogonal multiple access candidate for NR*, TSG RAN WG1 #85, Nanjing, China, May 2016, proposed by Samsung.

[20] K. Li, X. Wang, and L. Ping, "Analysis and optimization of interleave-division multiple-access communication systems," *IEEE Trans. Wireless Commun.*, vol. 6, no. 5, May 2007.

[21] L. Ping, L. Liu, K. Wu, and W. K. Leung, "Interleave division multiple-access," *IEEE Trans. Wireless Commun.*, vol. 5, no. 4, pp. 938–947, 2006.

[22] R. Hoshyar, F. Wathan, and R. Tafazolli, "Novel Low-Density Signature for Synchronous CDMA Systems over AWGN channel," *IEEE Trans. Signal Process.*, vol. 56, no. 4, pp. 1616–1626, Apr. 2008.

[23] G. C. Ferrante and M.-G. Di Benedetto, "Spectral efficiency of random time-hopping CDMA," *IEEE Trans. Inf. Theory*, vol. 61, no. 12, pp. 6643–6662, Dec. 2015.

[24] M. T. P. Le, G. C. Ferrante, T. Q. S. Quek, and M.-G. Di Benedetto, "Fundamental Limits of Low-Density Spreading NOMA with Fading," *IEEE Trans. Wireless Commun.*, 2018.

[25] X. Dai, S. Chen, S. Sun, S. Kang, Y. Wang, Z. Shen, and J. Xu, "Successive interference cancelation amenable multiple access (SAMA) for future wireless communications," in *Proc. IEEE Int. Conf. Commun. Sys. (ICCS)*, Macau, 2014, pp. 222–226.

[26] J. Choi, "Low density spreading for multicarrier systems," in *Spread Spectrum Techniques and Applications, 2004 IEEE Eighth International Symposium on*, 2004, pp. 575–578.

[27] L. Wen, R. Razavi, M. Imran, and P. Xiao, "Design of joint sparse graph for ofdm (jsg-ofdm) system," *IEEE Trans. Wireless Commun.*, vol. 14, no. 4, pp. 1823–1836, Apr. 2015.

[28] H. Nikopour and H. Baligh, "Sparse code multiple access," in *Proc. IEEE Annu. Int. Symp. Personal, Indoor, and Mobile Radio Commun. (PIMRC)*, London, UK, 2013, pp. 332–336.

[29] M. Zhao, S. Zhou, W. Zhou, and J. Zhu, "An Improved Uplink Sparse Coded Multiple Access," *IEEE Commun. Lett.*, vol. 21, no. 1, pp. 176–179, Jan. 2017.

[30] 3rd Generation Partnership Project (3GPP), *Low code rate and signature based multiple access scheme for New Radio*, TSG RAN1 #85, Nanjing, China, May 2016.

[31] ——, *Considerations on DL/UL multiple access for NR*, TSG RAN WG1 #84bis, Busan, Korea, Apr. 2016.

[32] ——, *Non-orthogonal multiple access for New Radio*, TSG RAN WG1 #85, Nanjing, China, May 2016, proposed by Nokia, Alcatel-Lucent Shanghai Bell.

[33] ——, *New uplink non-orthogonal multiple access schemes for NR*, TSG RAN WG1 #86, Gothenburg, Sweden, Aug. 2016.

[34] J. Zhang, X. Wang, X. Yang, and H. Zhou, "Low density spreading signature vector extension (lds-sve) for uplink multiple access," in *Proc. IEEE Veh. Technol. Conf. (VTC-Spring)*, Toronto, Canada, 2017, pp. 1–5.

[35] S. D. Sosnin, G. Xiong, D. Chatterjee, and Y. Kwak, "Non-Orthogonal Multiple Access with Low Code Rate Spreading and Short Sequence Based Spreading," 2017, pp. 1–5.

[36] 3rd Generation Partnership Project (3GPP), *Initial views and evaluation results on non-orthogonal multiple access for NR uplink*, TSG RAN WG1 #84bis, Busan, Korea, Apr. 2016.

[37] ——, *Candidate NR multiple access schemes*, TSG RAN WG1 #84bis, Busan, Korea, Apr. 2016.

[38] S. Verdú and S. Shamai, "Spectral efficiency of CDMA with random spreading," *IEEE Trans. Inf. Theory*, vol. 45, no. 2, pp. 622–640, Mar. 1999.

[39] X. Dai, Z. Zhang, S. Chen, S. Sun, and B. Bai, "Pattern Division Multiple Access (PDMA): A New Multiple Access Technology for 5G," *IEEE Wireless Commun. Mag.*, vol. 25, no. 2, pp. 54–60, Apr. 2018.

[40] A. M. Tulino, L. Li, and S. Verdú, "Spectral efficiency of multicarrier CDMA," *IEEE Trans. Inf. Theory*, vol. 51, no. 2, pp. 479–505, Feb. 2005.

[41] A. Montanari and D. N. C. Tse, "Analysis of belief propagation for non-linear problems: The example of CDMA (or: How to prove tanaka's formula)," in *Proc. IEEE Inf. Theory Workshop (ITW)*, Punta del Este, 2006, pp. 160–164.

[42] M. Yoshida and T. Tanaka, "Analysis of sparsely-spread CDMA via statistical mechanics," in *Proc. IEEE Int. Symp. Inf. Theory (ISIT)*, 2006, pp. 2378–2382.

[43] D. Guo and C.-C. Wang, "Multiuser detection of sparsely spread CDMA," *IEEE J. Sel. Areas Commun.*, vol. 26, no. 3, pp. 421–431, Apr. 2008.